Journal of Organometallic Chemistry 695 (2010) 137–144

Contents lists available at ScienceDirect

Journal of Organometallic Chemistry

journal homepage: www.elsevier.com/locate/jorganchem

A series of multinuclear homo- and heterometallic complexes with bridging tellurolato ligands derived from [Cp*Ir(CO)(TeTol)$_2$] (Cp* = η^5-C$_5$Me$_5$, Tol = *p*-tolyl)

Takafumi Nakagawa, Hidetake Seino, Yasushi Mizobe *

Institute of Industrial Science, The University of Tokyo, Komaba, Meguro-ku, Tokyo 153-8505, Japan

ARTICLE INFO

Article history:
Received 12 August 2009
Received in revised form 17 September 2009
Accepted 25 September 2009
Available online 4 October 2009

Keywords:
Iridium
Tellurolato complex
Multinuclear complex
Heterometallic complex
X-ray crystallography

ABSTRACT

Reactions of [Cp*Ir(CO)(TeTol)$_2$] (**1**; Tol = *p*-tolyl) with certain organometallic Pd(II), Pt(II), Ir(III), Rh(III), and Ru(II) species afforded IrPd, IrPt, IrPt$_2$, Ir$_2$, IrRh, IrRu$_3$, and IrRu complexes having tellurolato-bridged dinuclear or trinuclear cores. This finding demonstrates that **1** is a versatile precursor to synthesize a variety of multinuclear homo- and heterometallic μ-tellurolato complexes, whose chemistry is still less advanced as compared with that of μ-thiolato complexes.

1. Introduction

In contrast to the extensive studies that are continuing about the syntheses and reactivities of the alkoxido and thiolato complexes, the chemistry of heavier chalcogenolato, viz. selenolato and tellurolato complexes is less advanced [1]. Thus, with respect to the multinuclear complexes with bridging tellurolato ligands, for example, fully characterized compounds are relatively limited and those with the heterometallic cores are rare [2]. In this paper, we wish to describe the synthesis and structures of some new homometallic and heterobimetallic complexes with bridging tellurolato ligands derived from the bis(tellurolato) complex [Cp*Ir(CO)(TeTol)$_2$] (**1**; Cp* = η^5-C$_5$Me$_5$, Tol = *p*-tolyl) prepared previously in this laboratory [3].

2. Results and discussion

2.1. Reactions of *1* with Pd(II) and Pt(II) complexes

In the previous paper [3], we have reported the formation of the triangular clusters with two capping tellurido ligands [Cp*Ir(CO)(μ$_3$-Te)$_2${M(Tol)(PPh$_3$)}$_2$] (M = Pd, Pt) from **1** and 2 equiv. of [Pd(PPh$_3$)$_4$] or [Pt(PPh$_3$)$_3$]. These reactions proceed via the insertion of M(0) centers into Te–Tol bonds in **1**, and the expected intermediate stage [Cp*Ir(CO)(μ-Te)(μ-TeTol)Pt(Tol)(PPh$_3$)] was isolable from the reaction of **1** with 1 equiv. of [Pt(PPh$_3$)$_3$] (Scheme 1).

Now we have found that when **1** is allowed to react with an equimolar amount of Pd(II) complex [PdCl$_2$(cod)] (cod = 1,5-cyclooctadiene) at room temperature, the tellurolato-bridged heterobimetallic complex [Cp*Ir(CO)(μ-TeTol)$_2$PdCl$_2$] (**2**) is obtained in moderate yield (Eq. (1)). The structure of **2** has been determined by the X-ray crystallography. The ORTEP drawing is shown in Fig. 1, while the selected interatomic distances and angles are listed in Table 1.

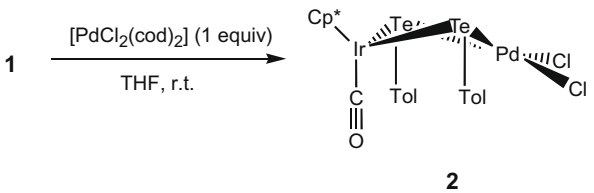

(1)

2

Complex **2** consists of the Ir and Pd centers with three-legged piano stool and square planar configurations, respectively, which are bridged by two TeTol ligands. The Ir–Pd distance at 3.9038(6) Å is indicative of the absence of any bonding interactions between these two metal centers. The IrPdTe$_2$ core is slightly folded with the dihedral angle of 165° around the Te···Te vector. Two Tol groups are mutually syn, which are oriented to the direction opposite to the bulky Cp* ligand. The Ir–Te, Pd–Te, and Pd–Cl bond lengths in **2** are not unusual. The ^{1}H NMR spectrum showing one Cp* resonance at δ 2.20 as well as one Me signal due to Tol

* Corresponding author. Fax: +81 3 5452 6361.
E-mail address: ymizobe@iis.u-tokyo.ac.jp (Y. Mizobe).

0022-328X/$ - see front matter © 2009 Elsevier B.V. All rights reserved.
doi:10.1016/j.jorganchem.2009.09.038

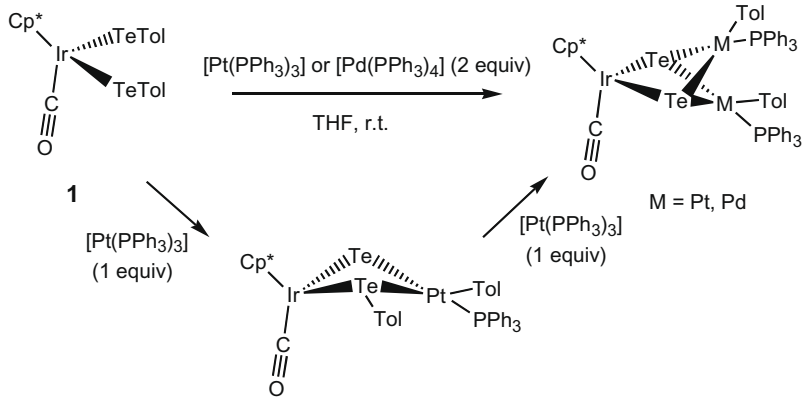

Scheme 1.

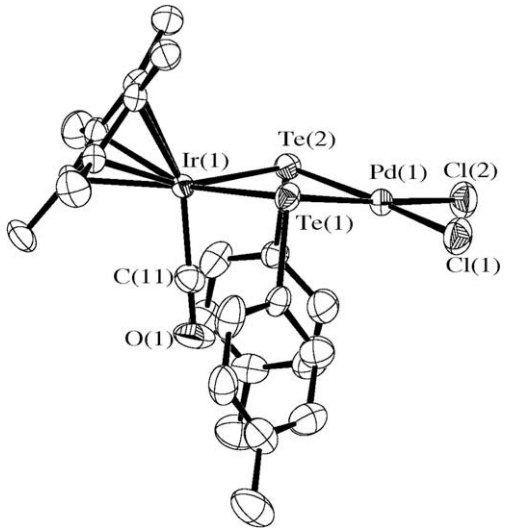

Fig. 1. An ORTEP drawing for **2** at 50% probability level. All hydrogen atoms are omitted for clarity.

groups at δ 2.27 is consistent with the solid structure. The ν(C≡O) value at 2023 cm^{-1} is somewhat higher than that in mononuclear **1** at 1982 cm^{-1} due to the weaker back-donating ability of the Ir center in **2** with μ-TeTol ligands than that in **1** with the terminal TeTol ligands.

The reaction of **1** with 1 equiv. of [$PtCl_2$(cod)] was conducted analogously, yielding the mixture of two products: a dinuclear complex [$Cp^*Ir(CO)(\mu\text{-TeTol})_2PtCl_2$] (**3**) and a trinuclear complex [{$Cp^*Ir(CO)(\mu\text{-TeTol})_2$}$_2$Pt]$Cl_2$ (**4**), the molar ratio of which in the reaction mixture was estimated to be ca. 5:3 from its ^{1}H NMR spectrum (Eq. (2)). Complex **4** was isolated as analytically pure crystals by recrystallizing the product mixture from DMF–ether, and the preliminary X-ray analysis disclosed its tellurolato-bridged trinuclear structure shown in Eq. (2). On the other hand, purification of **3** was unsuccessful despite the repeated crystallization of the evaporated residue of the mother liquor obtained after deposition of **4** on recrystallization. However, a small amount of single crystals formulated as **3**·$C_2H_4Cl_2$ ($C_2H_4Cl_2$ = 1,2-dichloroethane) were obtained during the attempts of purification and its structure could be determined in detail by the X-ray diffraction (Fig. 2). Selected bond distances and angles are summarized in Table 1.

Table 1
Selected interatomic distances (Å) and angles (°) in **2** and **3**.

2			
(a) Distances			
Ir···Pd	3.9038(6)		
Ir–Te(1)	2.6566(5)	Ir–Te(2)	2.6701(4)
Ir–C(11)	1.858(5)	C(11)–O(1)	1.135(7)
Pd–Te(1)	2.5184(6)	Pd–Te(2)	2.5434(6)
Pd–Cl(1)	2.371(2)	Pd–C1(2)	2.367(2)
(b) Angles			
Te(1)–Ir–Te(2)	78.98(1)	Te(1)–Pd–Te(2)	84.01(2)
Ir–Te(1)–Pd	97.89(2)	Ir–Te(2)–Pd	96.93(2)
Ir–Te(1)–C(12)	100.5(2)	Ir–Te(2)–C(19)	98.7(2)
Pd–Te(1)–C(12)	102.2(1)	Pd–Te(2)–C(19)	102.9(2)
Te(1)–Pd–Cl(1)	88.77(4)	Te(2)–Pd–Cl(2)	91.08(5)
Cl(1)–Pd–Cl(2)	96.17(6)	Ir–C(11)–O	177.7(5)
3			
(a) Distances			
Ir···Pt	3.8527(4)		
Ir–Te	2.6495(4)	Ir–C(7)	1.860(8)
C(7)–O(1)	1.152(10)	Pt–Te	2.5227(4)
Pt–Cl	2.351(1)		
(b) Angles			
Te–Ir–Te*	81.15(2)	Te–Pt–Te*	86.18(2)
Ir–Te–Pt	96.27(2)	Ir–Te(1)–C(1)	103.2(2)
Pt–Te–C(1)	102.5(1)	Te–Pt–Cl	90.10(3)
Cl–Pt–Cl*	93.58(5)	Ir–C(7)–O	178.9(7)

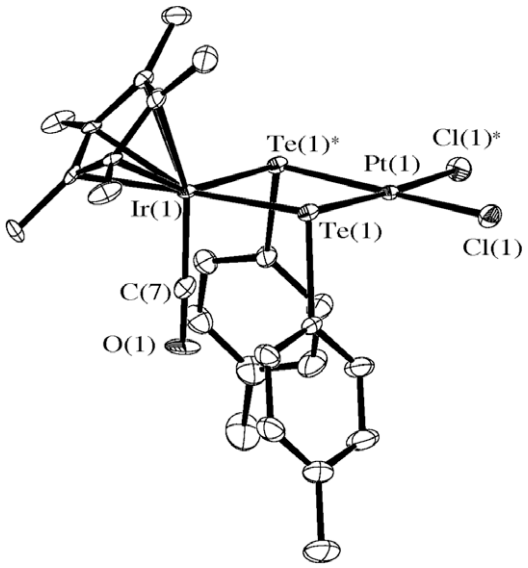

Fig. 2. An ORTEP drawing for **3** at 50% probability level. All hydrogen atoms are omitted for clarity. Crystallographically imposed mirror plane defined by the Ir and Pt centers as well as the CO ligand is present.

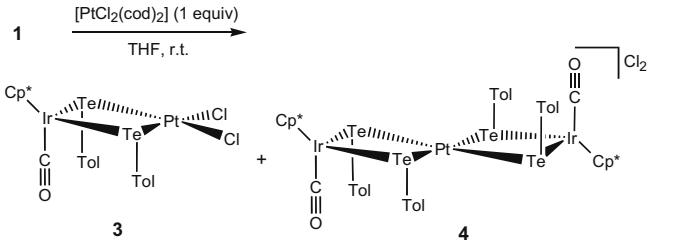

(2)

The crystal structure of **3** is essentially the same as that of **2**, except that the $IrPtTe_2$ ring is almost planar with the dihedral angle of 176° between the $IrTe_2$ and $PtTe_2$ planes around the Te···Te vector. The Ir···Pt separation at 3.8527(4) Å is indicative of the absence of any bonding interactions.

For **4**, the preliminary X-ray diffraction study has disclosed its trinuclear structure shown in Eq. (2). In **4**, the Pt atom coincides with the inversion center and the half of the molecule is crystallographically independent, the core structure of which is analogous to those in **3** and **2**. The ^1H NMR data as well as the ν(C≡O) value for **3** and **4** are diagnostic of these crystal structures (see Section 3).

2.2. Reactions of *1* with Ir(III) and Rh(III) complexes

Reactions of **1** with 0.5 equiv. of dinuclear Ir(III) and Rh(III) complexes $[(Cp^*MCl)_2(\mu\text{-}Cl)_2]$ were carried out in CH_2Cl_2 at room temperature, which afforded the mixtures of the tellurolato-bridged dinuclear complexes, *cis*-$[Cp^*Ir(CO)(\mu\text{-}TeTol)_2MCp^*Cl]Cl$ (M = Ir (**5a**), Rh (**6a**)) and their *trans*-isomers (M = Ir (**5b**), Rh (**6b**)) with respect to the disposition of two Cp^* ligands. The ratios **5a**:**5b** and **6a**:**6b** in the reaction mixtures determined by the NMR spectra were ca. 5:2 and 7:5, respectively (vide infra). The anion metathesis using KPF_6 in CH_2Cl_2 afforded the mixture of *cis*-$[Cp^*Ir(CO)(\mu\text{-}TeTol)_2IrCp^*Cl][PF_6]$ (**5′a**) and its *trans*-isomer (**5′b**) in ca. 5:2 ratio (Scheme 2), both of which were obtained as single crystals and characterized by the X-ray analysis using the crystals separated manually.

For the Ir–Rh complex **6**, the X-ray structure could be determined for **6a**, since the suitable single crystals were available only for **6a** from the mixture of the products **6a** and **6b**. Strangely, when this mixture was treated similarly with KPF_6, *cis*-$[Cp^*Ir(CO)(\mu\text{-}TeTol)_2RhCp^*Cl][PF_6]$ (**6′a**) was present as the sole complex in the reaction mixture. Thus, **6′a** was able to be isolated as an analytically pure form. The ORTEP drawings of the cations in **5′a**, **5′b**, and **6a** were depicted in Figs. 3–5, while important interatomic distances and angles therein are listed in Table 2.

As shown in Fig. 3, the solid state structure of **5′a** consists of the Ir_2Te_2 core, which is puckered only slightly with the dihedral angle between two $IrTe_2$ planes at 172°. The Ir···Ir separation at 3.964(1) Å indicates the absence of metal–metal bond. The geometry of the two Cp^* ligands is *cis* with respect to the Ir_2Te_2 ring, while that of the two Tol groups is *syn* and oriented to the direction opposite to the Cp^* ligands. Two benzene rings are close to parallel to the Ir···Ir vector, minimizing the steric repulsion between the Tol group and the CO and Cl ligands as well as the other Tol ligand.

The solid state structure of **5′b** is shown in Fig. 4, which clearly indicates the two Cp^* ligands in *trans* dispositions. The Ir_2Te_2 ring is almost planar with the dihedral angle around the Te···Te vector of 174° and the Ir···Ir distance without metal–metal bond is 3.9742(8) Å. Two Tol groups are *syn* and oriented to the direction of the CO ligand. In contrast to **5′a**, two Tol planes are close to perpendicular to the Ir···Ir vector, presumably because the steric repulsion against the Cp^* ligand is more significant than that to the other Tol group.

The X-ray structure of **6a** shown in Fig. 5 is quite similar to that of **5′a**, where the Ir···Rh distance is 3.971(1) Å and the dihedral angle between the $IrTe_2$ and $RhTe_2$ planes is 174°.

When the isolated crystals of **5′a**, **5′b**, and **6′a** were re-dissolved in $CDCl_3$, the NMR spectrum of each complex shows the presence of two species in solution as summarized in Section 3. This feature can be interpreted in terms of the equilibration of *syn* and anti forms with respect to the two Tol groups in a solution state, as is ubiquitously observed for the thiolato-bridged dinuclear cores [4]. The structures of *syn* and anti forms in equilibrium are depicted in Eqs. (3) and (4), the ratios of which were 15:4, 5:3, and 1:1, for **5′a**, **5′b**, and **6′a**, respectively. Since the chemical shifts of the signals observed for the *syn* and anti forms for **5′a**, **5′b**, and **6′a** are in good agreement with those of the spectra for the complexes having the Cl counter anions **5** and **6**, the ratios of **5a**/**5b** and **6a**/**6b** in the reaction mixtures shown in Scheme 2 could be determined from the NMR criteria (vide supra, see also the Section 3).

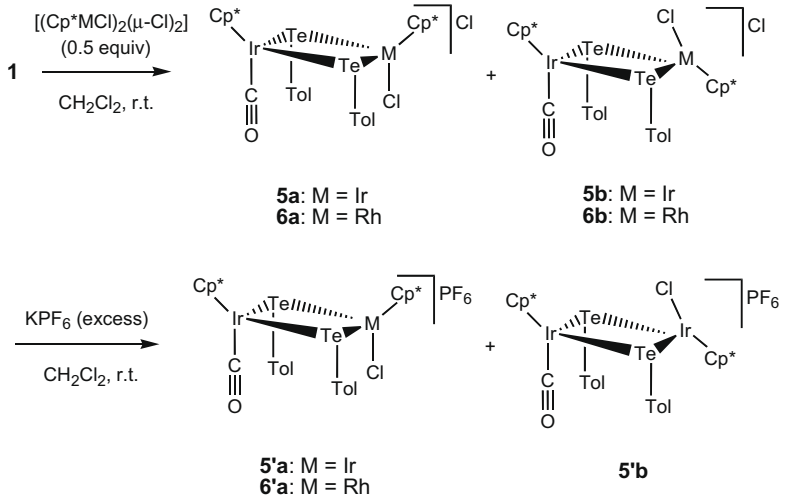

Scheme 2.

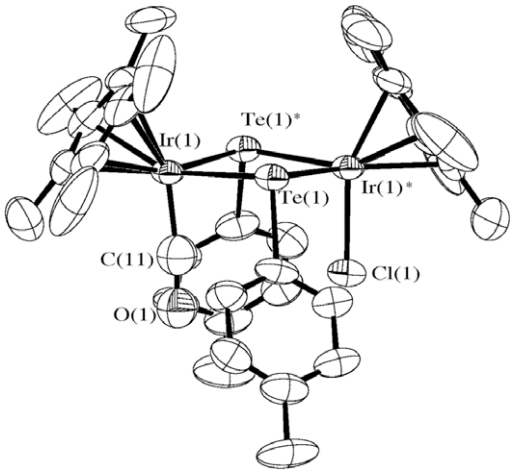

Fig. 3. An ORTEP drawing of the cation of **5′a** at 50% probability level. All hydrogen atoms are omitted for clarity. A half of this structure is crystallographically independent, which includes the CO and Cl ligands disordered with the 50:50 occupancies.

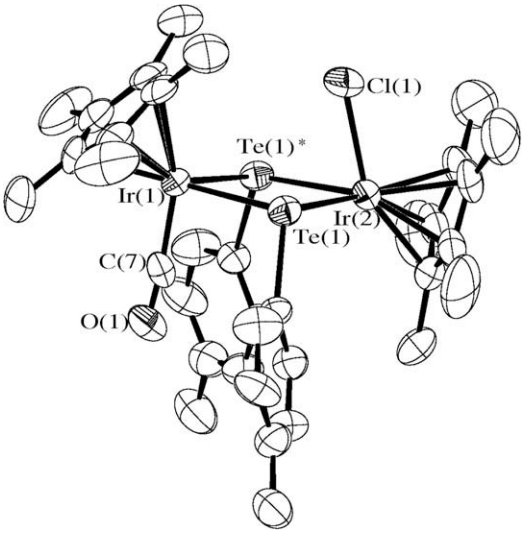

Fig. 4. An ORTEP drawing of the cation of **5′b** at 50% probability level. All hydrogen atoms are omitted for clarity. Crystallographic mirror plane is present including two Ir centers as well as the CO and Cl ligands.

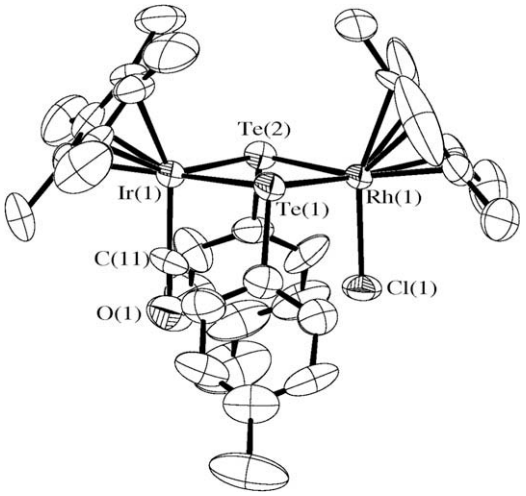

Fig. 5. An ORTEP drawing of the cation of **6a** at 50% probability level. All hydrogen atoms are omitted for clarity.

Table 2
Selected interatomic distances (Å) and angles (°) in **5′a**, **5′b**, and **6′a**.

5′a			
(a) Distances			
Ir···Ir*	3.964(1)		
Ir–Te	2.6346(8)	Ir–Te*	2.6287(7)
Ir–Cl	2.336(7)	Ir–C(11)	1.83(2)
C(11)–O	1.15(2)		
(b) Angles (°)			
Te–Ir–Te*	81.76(2)	Ir–Te–Ir*	92.88(2)
Ir–Te–C(12)	104.4(3)	Ir*–Te–C(12)	107.2(3)
Ir–C(11)–O	174(2)		
5′b			
(a) Distances			
Ir(1)···Ir(2)	3.9742(8)		
Ir(1)–Te	2.6425(8)	Ir(2)–Te	2.6409(8)
Ir(1)–C(7)	1.85(2)	Ir(2)–Cl	2.429(4)
C(7)–O	1.14(2)		
(b) Angles (°)			
Te–Ir(1)–Te*	82.22(2)	Te–Ir(2)–Te*	82.28(2)
Ir(1)–Te–Ir(2)	97.56(2)	Ir(1)–Te–C(8)	105.2(2)
Ir(2)–Te–C(8)	110.9(2)	Ir(1)–C(7)–O	175(1)
6′a			
(a) Distances			
Ir···Rh	3.9702(6)		
Ir–Te(1)	2.6339(6)	Rh–Te(1)	2.6301(8)
Ir–Te(2)	2.6371(7)	Rh–Te(2)	2.6244(8)
Ir–C(11)	1.861(7)	Rh–Cl(1)	2.366(2)
C(11)–O	1.123(8)		
(b) Angles (°)			
Te(1)–Ir–Te(2)	81.74(2)	Te(1)–Rh–Te(2)	82.05(2)
Ir–Te(1)–Rh	97.91(2)	Ir–Te(2)–Rh	97.98(2)
Ir–Te(1)–C(12)	103.7(2)	Rh–Te(1)–C(12)	110.7(2)
Ir–Te(2)–C(19)	105.9(2)	Rh–Te(2)–C(19)	109.5(2)
Ir–C(11)–O	178.2(6)		

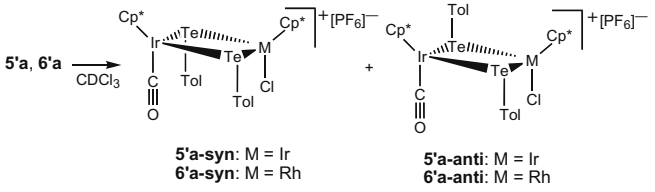

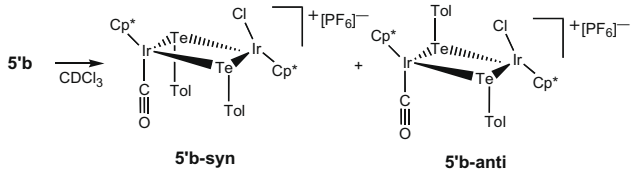

(3)

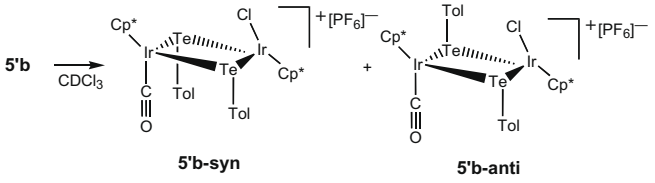

(4)

2.3. Reactions of **1** with Ru(II) complexes

Treatment of **1** with 0.25 equiv. of $[(Cp^*Ru)_4(\mu_3\text{-}Cl)_4]$ in CH_2Cl_2 at room temperature resulted in the formation of the mixture, the NMR spectrum of which showed the presence of four isomers as observed for the reactions of **1** with $[(Cp^*MCl)_2(\mu\text{-}Cl)_2]$ (M = Ir,

Rh) described above. This presumably suggests that the reaction proceeds analogously, affording the tellurolato-bridged dinuclear Ir–Ru complexes with *cis* and *trans* forms that are convertible to the *syn* and anti forms in solutions. However, the product from this reaction was not isolable in a pure form to be subjected for full characterization.

Interestingly, when **1** was allowed to react with 0.75 equiv. of $[(Cp^*Ru)_4(\mu_3\text{-}Cl)_4]$ in CH_2Cl_2 at room temperature, a tetranuclear complex $[Cp^*IrCl\{\mu\text{-}Te(\eta^6\text{-}Tol)RuCp^*\}_2RuCp^*(CO)]Cl_2$ (**7**) was obtained in moderate yield. Preparation of the single crystals was attempted by converting **7** to $[Cp^*IrCl\{\mu\text{-}Te(\eta^6\text{-}Tol)RuCp^*\}_2RuCp^*(CO)][PF_6]_2$ (**7′**) through the metathetical reaction with KPF_6. However, due to the poor quality of the crystals, the X-ray analysis was unable to be completed. Nevertheless, it disclosed the atom connectivities in **7′** (Scheme 3).

Complex **7′** has a dinuclear core bridged by two TeTol ligands, where the dispositions of two Cp^* ligands and two Tol groups are *cis* and syn, respectively. There are no bonding interactions between Ir and Ru centers. Two Tol planes are oriented parallel to the Ir–Ru vector and the Cp^*Ru fragment binds to each of the benzene rings of the μ-TeTol ligands, forming (π-Cp^*)Ru(π-arene) chromophore. The ^1H NMR spectrum of **7** is consistent with this solid state structure. Characteristic high-field shifts of the resonances due to the aryl protons of Tol groups in the ^1H NMR spectrum (δ = 5.4–5.9) are diagnostic of the π-coordination to the Cp^*Ru center. Unfortunately, since the Ir and Ru sites are disordered with ca. 50:50 occupancies, the ligand bonded to each metal, viz., either Cl or CO, could not be determined crystallographically. However, the ν(C≡O) value of 1937 cm^{-1} observed for **7**, which is lower by 85–93 cm^{-1} than those observed for the CO ligands bound to the Ir(III) centers in **2**–**6**, indicates presumably that the CO is bonded to the Ru center in **7′**. In relation to this assignment, it is to be noted, for example, that $[CpRu(CO)(PPh_3)(SC_6F_5)]$ [6] and $[Cp^*Ir(CO)(SPh)_2]$ [7] show ν(CO) bands at 1956 and 1994 cm^{-1}, respectively.

The reaction of **1** with an equimolar amount of the Ru(II) complex $[RuH(cod)(MeCN)_3][BPh_4]$ resulted in the formation of the dinuclear complex $[Cp^*Ir(\mu\text{-}H)(\mu\text{-}TeTol)_2Ru(CO)(cod)][BPh_4]$ (**8**) in moderate yield (Eq. (5)). The X-ray diffraction study has disclosed its structure in detail as shown in Fig. 6 and Table 3.

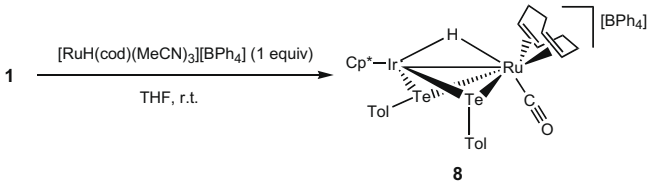

(5)

Complex **8** has a bimetallic core bridged by two TeTol ligands, where the geometry of two Tol groups is anti with one axial and one equatorial orientations. The Ir···Ru distance at 2.9038(4) Å indicates the presence of bonding interactions between two metal centers. This resulted in the Ir–μ-Te bond distances at 2.6051(4) and 2.6145(4) Å slightly or considerably shorter than those in **2**, **3**, **5′**, and **6′** without metal–metal bond (2.63–2.67 Å). For comparison, the Ir–Te bond lengths for the TePh ligand bridging to the Ir–Ir bond in the clusters $[Ir_6(CO)_{14}(\mu\text{-}TePh)]^-$ and $[Ir_6(CO)_{13}(\mu\text{-}TePh)_2]$ are 2.60–2.63 Å [5]. Although the hydride was unable to be located from the Fourier map, appearance of the singlet resonance at δ −14.3 in the ^1H NMR spectrum unambiguously indicated the existence of the hydride ligand. The dihedral angle between two IrRuTe planes at 106.4° suggests that the hydride is presumably bridging the Ir–Ru bond to give the triply bridged Ir–Ru core. As in **7** and **7′**, migration of the CO ligand from Ir to Ru occurred also in **8**. The ν(C≡O) value of 1994 cm^{-1} is significantly higher than that in **7**.

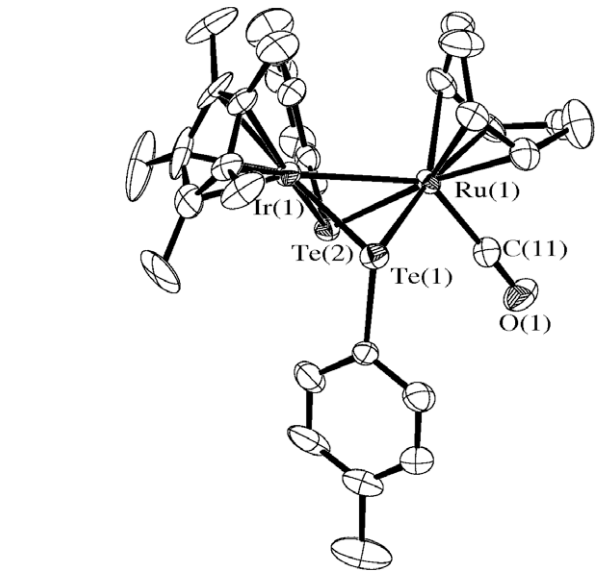

Fig. 6. An ORTEP drawing of the cation of **8** at 50% probability level. All hydrogen atoms are omitted for clarity.

Table 3
Selected interatomic distances (Å) and angles (°) in **8**.

(a) Distances			
Ir–Ru	2.9037(5)		
Ir–Te(1)	2.6048(4)	Ir–Te(2)	2.6147(4)
Ru–Te(1)	2.6348(6)	Ru–Te(2)	2.6512(5)
Ru–C(11)	1.898(6)	C(11)–O	1.135(8)
(b) Angles (°)			
Te(1)–Ir–Te(2)	84.36(1)	Te(1)–Ru–Te(2)	83.07(2)
Ir–Te(1)–Ru	67.31(1)	Ir–Te(2)–Ru	66.93(1)
Ir–Te(1)–C(12)	110.3(2)	Ir–Te(2)–C(19)	107.8(2)
Ru–Te(1)–C(12)	104.9(2)	Ru–Te(2)–C(19)	107.7(2)
Ru–C(11)–O	178.5(5)		

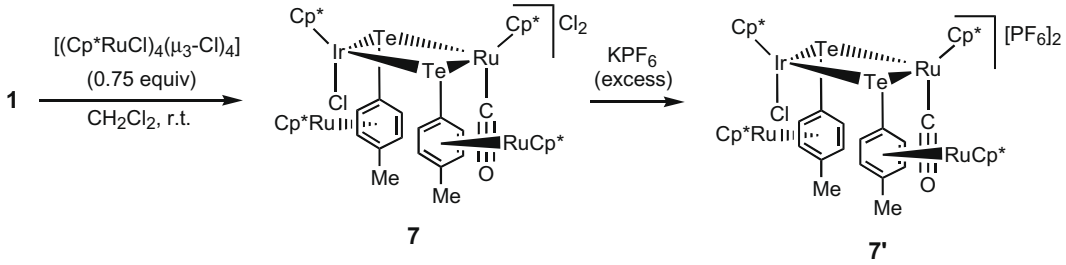

Scheme 3.

3. Experimental

3.1. General

All manipulations were carried out under N_2 using standard Schlenk techniques. Solvents were dried by common methods and distilled under N_2 before use. Complexes **1** [3], $[MCl_2(cod)]$ (M = Pd [8], Pt [9]), $[(Cp^*MCl)_2(\mu\text{-}Cl)_2]$ (M = Ir, Rh) [10], $[(Cp^*Ru)_4(\mu_3\text{-}Cl)_4]$ [11], and $[RuH(cod)(MeCN)_3][BPh_4]$ [12] were prepared according to the literature methods, while KPF_6 was obtained commercially and used as received.

IR and NMR spectra were recorded on a JASCO FT/IR-420 and a JEOL alpha-400 spectrometer, respectively. Elemental analyses were done with a Perkin–Elmer 2400 series II CHN analyzer.

3.2. Preparation of **2**

A THF solution (5 cm^3) containing **1** (40 mg, 0.050 mmol) and $[PdCl_2(cod)]$ (15 mg, 0.050 mmol) was stirred at room temperature. The mixture changed immediately to an yellow suspension, which was filtered off and the remained solid was extracted with DMF. Addition of ether to the concentrated extract afforded yellow crystals of **2** (32 mg, 66% yield). IR (KBr): 2023 ($\nu_{C\equiv O}$) cm^{-1}. ^1H NMR (DMSO-d_6): δ 2.20 (s, 15H, Cp^*), 2.27 (s, 6H, C_6H_4Me), 7.05, 7.92 (d, J = 8.4 Hz, 4H each, C_6H_4). Anal. Calc. for $C_{25}H_{29}OCl_2PdTe_2Ir$: C, 30.95; H, 3.01. Found: C, 31, 17; H, 3.09%.

3.3. Preparation of **3** and **4**

After stirring the mixture of **1** (16 mg, 0.020 mmol) and $[PtCl_2(cod)]$ (7.5 mg, 0.020 mmol) in THF (5 cm^3) at room temperature, the suspension was obtained immediately, which was filtered off. The ^1H NMR spectrum of the remained solid showed the presence of two products, **3** and **4**, in a molar ratio 3:5. Crystallization of this solid using DMF–ether afforded only **4** as analytically pure, yellow crystals (11 mg, 59% yield based on Ir). The results of the preliminary X-ray analysis disclosed the atom-connecting scheme in **4**. Complex **4**: IR (KBr): 2022 ($\nu_{C\equiv O}$) cm^{-1}. ^1H NMR (DMSO-d_6): δ 2.07 (s, 30H, Cp^*), 2.34 (s, 12H, C_6H_4Me), 7.11, 7.75 (d, J = 8.0 Hz, 8H each, C_6H_4). Anal. Calc. for $C_{50}H_{58}O_2Cl_2Te_4Ir_2Pt$: C, 32.43; H, 3.15. Found: C, 32.11; H, 3.13%. Complex **3** was obtained by recrystallizing the evaporated residue of the mother liquor from CH_2Cl_2–hexane but in the impure form and could not be isolated in the analytically pure state despite the repeated crystallization. The structure of **3** was confirmed by using the single crystals of **3**·$C_2H_4Cl_2$ deposited in a small amount upon crystallization from $C_2H_4Cl_2$–ether. Complex **3**: IR (KBr): 2022 ($\nu_{C\equiv O}$) cm^{-1}. ^1H NMR (DMSO-d_6): δ 2.18 (s, 15H, Cp^*), 2.30 (s, 6H, C_6H_4Me), 7.06, 7.89 (d, J = 8.0 Hz, 4H each, C_6H_4).

3.4. Preparation of **5** and **5′**

To a solution of **1** (918 mg, 1.15 mmol) in CH_2Cl_2 (30 cm^3) was added $[(Cp^*IrCl)_2(\mu\text{-}Cl)_2]$ (465 mg, 0.584 mmol) at room temperature. After stirring for 20 h, the resultant solution was concentrated in vacuo. Addition of hexane afforded spectroscopically pure **5** as orange powder (1.39 g, 92% yield). The NMR spectrum of the reaction mixture showed the presence of **5a** and **5b** in the ratio of 9:4.

A mixture of **5** (357 mg, 0.300 mmol) and KPF_6 (106 mg, 0.576 mmol) in CH_2Cl_2 (5 cm^3) was stirred at room temperature for 2 h and the resultant mixture was filtered. Addition of hexane to the concentrated filtrate gave **5′** as a mixture of **5′a** as platelike crystals and **5′b** as prismatic crystals in the combined yield of 316 mg (80% based on **5**). The NMR spectrum of the reaction mixture indicated the formations of **5′a** and **5′b** in the ratio of 5:2. The single-crystal X-ray analysis was performed for both **5′a** and **5′b**. The data below were obtained by using some crystals collected manually. Complex **5′a**: IR (KBr): 2030 ($\nu_{C\equiv O}$) cm^{-1}. Anal. Calc. for $C_{35}H_{44}OF_6PClTe_2Ir_2$: C, 32.31; H, 3.41. Found: C, 32.29; H, 3.41%. ^1H NMR ($CDCl_3$): δ 1.88, 2.21 (s, 15H each, Cp^*), 2.30 (s, 6H, C_6H_4Me), 6.98, 7.32 (d, J = 8.0 Hz, 4H each, C_6H_4) for **5′a-syn**; δ 1.58, 1.80 (s, 15H each, Cp^*), 2.35, 2.43 (s, 3H each, C_6H_4Me), 7.02, 7.64 (d, J = 8.0 Hz, 2H each, C_6H_4; the resonances for the remaining 4 protons were not assignable) for **5′a-anti**. The ratio of **5′a-syn** and **5′a-anti** was 15:4. Complex **5′b**: IR (KBr): 2030 ($\nu_{C\equiv O}$) cm^{-1}. Anal. Calc. for $C_{35}H_{44}OF_6PClTe_2Ir_2$: C, 32.31; H, 3.41. Found: C, 32.23; H, 3.40%. ^1H NMR ($CDCl_3$): δ 1.60, 2.09 (s, 15H each, Cp^*), 2.46 (s, 6H, C_6H_4Me), 7.18, 7.70 (d, J = 8.0 Hz, 4H each, C_6H_4) for **5′b-syn**; δ 1.63, 1.86 (s, 15H each, Cp^*), 2.21, 2.37 (s, 3H each, C_6H_4Me), 7.05, 7.11, 7.48, 7.54 (d, J = 8.0 Hz, 2H each, C_6H_4) for **5′b-anti**. The ratio of **5′b-syn** and **5′b-anti** was 5:3.

3.5. Preparation of **6** and **6′**

Complex **6** was obtained as spectroscopically pure, dark red powder from **1** (79 mg, 0.10 mmol) and $[(Cp^*RhCl)_2(\mu\text{-}Cl)_2]$ (31 mg, 0.050 mmol) by the analogous procedure to prepare **5** (81 mg, 73% yield). The NMR spectrum of the reaction mixture showed the presence of **6a** and **6b** in the ratio of 7:5. Single crystals of **6a**·$0.2CH_2Cl_2$·$0.4C_6H_{14}$ for the X-ray analysis were obtained from CH_2Cl_2–hexane.

Complex **6** (102 mg, 0.0926 mmol) was similarly converted to **6′** upon treatment with KPF_6 (35 mg, 0.19 mmol), which was obtained as dark red needles of **6′**·CH_2Cl_2 (84 mg, 75% yield based on **6**). The NMR spectrum of the reaction mixture disclosed the presence of only **6′a**. Complex **6′a**·CH_2Cl_2: IR (KBr): 2029 ($\nu_{C\equiv O}$) cm^{-1}. Anal. Calc. for $C_{36}H_{46}OF_6PCl_3RhTe_2Ir$: C, 33.35; H, 3.58. Found: C, 33.38; H, 3.59%. ^1H NMR ($CDCl_3$): δ 1.81, 2.20 (s, 15H each, Cp^*), 2.32 (s, 6H, C_6H_4Me), 7.00, 7.44 (d, J = 8.0 Hz, 4H each, C_6H_4) for **6′a-syn**; δ 1.55, 1.85 (s, 15H each, Cp^*), 2.36, 2.43 (s, 3H each, C_6H_4Me), 7.02, 7.73 (d, J = 8.0 Hz, 2H each, C_6H_4; the resonances for the remaining 4 protons were not assignable) for **6′a-anti**. The ratio of **6′a-syn** and **6′a-anti** was 1:1.

3.6. Preparation of **7** and **7′**

A mixture of **1** (80 mg, 0.10 mmol) and $[(Cp^*RuCl)_4(\mu_3\text{-}Cl)_4]$ (80 mg, 0.075 mmol) in CH_2Cl_2 (5 cm^3) was stirred at room temperature for 25 h. The resultant dark red solution was evaporated to dryness in vacuo and the residue was crystallized from $ClCH_2CH_2Cl$ and hexane, affording **7** as dark red crystals (95 mg, 58% yield). IR (KBr): 1937 ($\nu_{C\equiv O}$) cm^{-1}. ^1H NMR ($CDCl_3$): δ 1.91, 2.02 (s, 15H each, Cp^*), 1.99 (s, 30H, Cp^*Ru), 2.12 (s, 6H, C_6H_4Me), 5.47–5.49 (br, 4H, C_6H_4), 5.52, 5.83 (d, J = 6.0 Hz, 2H each, C_6H_4). In spite of the attempts to analytically pure **7**, satisfactory C and H analysis data were not obtained.

Single crystals of **7′** for the preliminary X-ray diffraction study were obtained by treating **7** with 3 equiv. of KPF_6 in CH_2Cl_2, followed by crystallization of the product from $C_2H_4Cl_2$–ether.

3.7. Preparation of **8**

To a solution of **1** (75 mg, 0.095 mmol) in THF (5 cm^3) was added $[RuH(cod)(MeCN)_3][BPh_4]$ (62 mg, 0.095 mmol) and the mixture was stirred at room temperature for 4 h. Addition of ether to the concentrated product solution gave **8** as dark red crystals (53 mg, 42% yield). IR (KBr): 1994 ($\nu_{C\equiv O}$) cm^{-1}. ^1H NMR ($CDCl_3$): δ −14.3 (s, 1H, μ-H), 1.91, 2.23 (s, 15H, Cp^*), 2.27, 2.38 (s, 3H each, C_6H_4Me), 2.0–2.6 (6H, CH_2 of cod), 2.67 (br, 2H, CH_2 of cod), 3.51, 3.61, 3.83, 4.50 (br, 1H each, CH of cod), 6.87, 6.89 (d, J = 8.0 Hz, 2H each, C_6H_4), 7.00–7.05 (4H, C_6H_4), 6.88 (t, J = 7.2 Hz, 4H, p-H

Table 4
Crystal data for **2**, **3**·$C_2H_4Cl_2$, **5′a-syn**, **5′b-syn**, **6a-syn**·C_6H_{14}, and **8**.

	2	**3**·$C_2H_4Cl_2$	**5′a-syn**	**5′b-syn**	**6a-syn**·0.2CH_2Cl_2·0.4C_6H_{14}	**8**
Formula	$C_{25}H_{29}OCl_2PdTe_2Ir$	$C_{27}H_{33}OCl_6Te_2IrPt$	$C_{35}H_{44}OF_6PClTe_2Ir_2$	$C_{35}H_{44}OF_6PClTe_2Ir_2$	$C_{37.6}H_{50}OCl_{2.4}RhTe_2Ir$	$C_{57}H_{62}BORuTe_2Ir$
Formula weight	970.23	1228.79	1300.79	1300.79	1153.42	1322.42
Space group	$P2_1/n$ (No. 14)	$P2_1/m$ (No. 11)	$P2_12_12$ (No. 18)	$I4/m$ (No. 87)	$P2_12_12_1$ (No. 19)	$P2_1/n$ (No. 14)
a (Å)	10.196(1)	9.774(2)	14.103(4)	21.208(1)	8.857(2)	11.470 (2)
b (Å)	22.581(3)	15.266(3)	15.882(4)	21.208(1)	15.095(3)	14.821(2)
c (Å)	12.606(2)	10.844(2)	9.082(3)	17.809(1)	31.425(7)	29.624(5)
β (°)	107.724(1)	95.398(1)	90	90	90	94.0274(5)
V (Å^3)	2764.6(5)	1610.8(6)	2022(1)	8010.0 (5)	4201(2)	5023(1)
Z	4	2	2	8	4	4
ρ_{calcd} (g cm^{-3})	2.33	2.53	2.14	2.16	1.82	1.75
Crystal size (mm^3)	0.30 × 0.30 × 0.20	0.20 × 0.10 × 0.10	0.60 × 0.30 × 0.15	0.40 × 0.30 × 0.15	0.40 × 0.30 × 0.15	0.40 × 0.10 × 0.03
Number of unique reflections	6283	3811	4632	4744	9625	11469
Number of data observed ($I > 2\sigma(I)$)	5246	2300	3295	2668	6662	8620
Number of variables	318	202	241	265	455	629
Transmission factor	0.121–0.212	0.028–0.341	0.105–0.294	0.094–0.290	0.283–0.465	0.583–0.883
R_1[a]	0.029	0.034	0.042	0.054	0.031	0.042
wR_2[b]	0.096	0.103	0.123	0.169	0.061	0.123
GOF[c]	1.02	1.02	1.02	1.03	1.04	1.02

[a] $R_1 = \Sigma||F_o| - |F_c||/\Sigma|F_o|$ ($I > 2\sigma(I)$).

[b] $wR_2 = [\sum(w(F_o^2 - F_c^2)^2)/\sum w(F_o^2)^2]^{1/2}$ (all data).

[c] GOF = $[\Sigma w(|F_o| - |F_c|)^2/\{(\text{no. observed}) - (\text{no. variables})\}]^{1/2}$.

of BPh_4), 7.03 (t, J = 7.2 Hz, 8H, m-H of BPh_4), 7.42 (br, 8H, o-H of BPh_4). Anal. Calc. for $C_{57}H_{62}OBRuTe_2Ir$: C, 51.77; H, 4.73. Found: C, 51.69; H, 4.15% (Table 4).

3.8. X-ray crystallography

Single crystals of **2**, **3**·2$C_2H_4Cl_2$, **5′a-syn**, **5′b-syn**, **6a-syn**·0.2CH_2Cl_2·0.4C_6H_{14}, and **8** were sealed in glass capillaries under argon and mounted on a Rigaku Mercury-CCD diffractometer equipped with a graphite-monochromatized Mo Kα source. Diffraction studies for **2**, **5′a-syn**, **5′b-syn**, and **8** were done at room temperature, while those for **3**·2$C_2H_4Cl_2$ and **6a-syn**·0.2CH_2Cl_2·0.4C_6H_{14} were at 113 K. Data collections were performed by using the CRYSTALCLEAR program package [13]. All data were corrected for Lorentz and polarization effects as well as absorption.

Structure solution and refinements were conducted by using the CRYSTALSTRUCTURE program package [14]. The positions of non-hydrogen atoms were determined by Patterson methods (PATTY) [15] and subsequent Fourier synthesis (DIRDIF99) [16], which were refined by full-matrix least-squares techniques using anisotropic thermal parameters. Hydrogen atoms were placed at the calculated positions and included at the final stages of the refinements with fixed parameters.

Preliminary X-ray results for **4**: formula, $C_{50}H_{58}Cl_2Ir_2O_2PtTe_4$; F_w = 1851.84; space group, $P2_1/n$ (no. 14); a = 10.555(9), b = 15.73(1), c = 17.98(2) Å, β = 96.051(4)°, V = 2967(4) Å^3; Z = 2; ρ_{calc} = 2.07 g cm^{-3}; crystal size, 0.40 × 0.10 × 0.10 mm^3; no of unique reflections, 5958; no of variables, 176; R_1 value using the data of $I > 2\sigma(I)$, 0.093; wR_2 value using all data, 0.28; GOF, 1.01. For **7′**·$C_2H_4Cl_2$: formula, $C_{56}H_{78}Cl_3F_{12}IrOP_2Ru_3Te_2$; F_w = 1914.15; space group, $P2_1/c$ (no. 14); a = 13.296(4), b = 14.500(4), c = 34.04(1) Å, β = 93.831(2)°, V = 6547(3) Å^3; Z = 4; ρ_{calc} = 1.94 g cm^{-3}; crystal size, 0.20 × 0.20 × 0.20 mm^3; no of unique reflections, 14 505; no of variables, 545; R_1 value using the data of $I > 2\sigma(I)$, 0.070; wR_2 value using all data, 0.21; GOF, 1.01.

Acknowledgements

This work was supported by Grant-in-Aid for Scientific Research on Priority Areas (No. 18065005, "Chemistry of Concerto Catalysis") and in part by Global COE Program "Chemistry Innovation through Cooperation of Science and Engineering" from the Ministry of Education, Culture, Sports, Science and Technology, Japan. Grant-in-Aid for JSPS Fellows (20-6569) is also appreciated (T.N.).

Appendix A. Supplementary material

CCDC 745322, 745323, 745324, 745325, 745326 and 745327 contain the supplementary crystallographic data for **5′b-syn**, **5′a-syn**, **6a-syn**, **2**, **8** and **3**. These data can be obtained free of charge from The Cambridge Crystallographic Data Centre via www.ccdc.cam.ac.uk/data_request/cif. Supplementary data associated with this article can be found, in the online version, at doi:10.1016/j.jorganchem.2009.09.038.

References

[1] (a) J. Arnold, Prog. Inorg. Chem. 43 (1995) 353;
(b) A.J. Singh, S. Sharma, Coord. Chem. Rev. 209 (2000) 49;
(c) M.C. Gimeno, in: F.A. Derillanova (Ed.), Handbook of Chalcogen Chemistry, RSC Publishing, Cambridge, UK, 2009, pp. 33–80.
[2] (a) S. Nagao, H. Seino, M. Hidai, Y. Mizobe, Dalton Trans. (2005) 3166;
(b) W.-F. Liaw, C.-Y. Chuang, W.-Z. Lee, C.-K. Lee, G.-H. Lee, S.-M. Peng, Inorg. Chem. 35 (1996) 2530;
(c) W.-F. Liaw, D.-S. Ou, Y.-S. Li, W.-Z. Lee, C.-Y. Chuang, Y.-P. Lee, G.-H. Lee, S.-M. Peng, Inorg. Chem. 34 (1995) 3747;
(d) A. Khanna, B.L. Khandelwal, S.K. Gupta, Transition Met. Chem. 19 (1994) 442.
[3] T. Nakagawa, H. Seino, S. Nagao, Y. Mizobe, Angew. Chem., Int. Ed. 45 (2006) 7758.
[4] (a) E.W. Abel, S.K. Bhargava, K.G. Orrell, Prog. Inorg. Chem. 32 (1984) 1;
(b) M. Hidai, Y. Mizobe, H. Matsuzaka, J. Organomet. Chem. 473 (1994) 1.
[5] R.D. Pergola, A. Ceriotti, A. Cinquantini, F.F. de Biani, L. Garlaschelli, M. Manassero, R. Piacentini, M. Sansoni, P. Zanello, Organometallics 17 (1998) 802.
[6] K. Shawakfeh, M. Wl-khateeb, D. Taher, H. Görls, W. Weigand, Transition Met. Chem. 33 (2008) 387.
[7] M. Herberhold, G.-X. Jin, A.L. Rheingold, J. Organomet. Chem. 570 (1998) 241.
[8] D. Drew, J.R. Doyle, Inorg. Synth. 13 (1972) 52.
[9] J.X. McDermott, J.F. White, G.M. Whitesides, J. Am. Chem. Soc. 98 (1976) 6521.
[10] C. White, A. Yates, P.M. Maitlis, Inorg. Synth. 29 (1992) 228.
[11] P.J. Fagan, M.D. Ward, J.C. Calabrese, J. Am. Chem. Soc. 111 (1989) 1698.
[12] T.V. Ashworth, R.H. Reimann, E. Singleton, J. Chem. Soc., Dalton Trans. (1978) 1036.
[13] CRYSTALCLEAR 1.3.6: Rigaku/MSC: 9009 New Trails Dr., The Woodlands, TX 77381, USA, 1998–2006.
[14] CRYSTALSTRUCTURE 3.8.0: Crystal structure analysis package, Rigaku and Rigaku/MSC: 9009 New Trails Dr., The Woodlands, TX 77381, USA, 2000–2006.;

CRYSTALS Issue 11: J.R. Carruthers, J.S. Rollett, P.W. Betteridge, D. Kinna, L. Pearce, A. Larsen, E. Gabe, Chemical Crystallography Laboratory, Oxford, UK, 1999.
[15] PATTY: P.T. Beurskens, G. Admiraal, G. Beurskens, W.P. Bosman, S. Garcia-Granda, R.O. Gould, J.M.M. Smits, C. Smykall, The DIRDIF program system, Technical Report of the Crystallography Laboratory, University of Nijmegen, The Netherlands, 1992.
[16] DIRDIF99: P.T. Beurskens, G. Admiraal, G. Beurskens, W.P. Bosman, R. de Gelder, R. Israel, J.M.M. Smits, The DIRDIF-99 program system, Technical Report of the Crystallography Laboratory, University of Nijmegen, The Netherlands, 1999.